Next Generation Neuropeptide Y Receptor Small Molecule Agonists Inhibit Mosquito Biting Behavior

Emely V. Zeledon[1, 2], Leigh A. Baxt[3], Tanweer A. Khan[3], Mayako Michino[3], Michael Miller[3], David J. Huggins[3,4], Caroline S. Jiang[5], Leslie B. Vosshall[1,2,6], Laura B. Duvall[7,8]

[1]Laboratory of Neurogenetics and Behavior, The Rockefeller University, New York NY 10065, USA
[2]Howard Hughes Medical Institute, New York NY 10065, USA
[3]Sanders Tri-Institutional Therapeutics Discovery Institute, New York, New York 10065, USA
[4]Department of Physiology and Biophysics, Weill Cornell Medicine, New York NY 10065, USA
[5]Center for Clinical and Translational Science, The Rockefeller University, New York, NY 10065, USA
[6]Kavli Neural Systems Institute, New York, NY 10065, USA
[7]Department of Biological Sciences, Columbia University, New York NY 10027, USA
[8]Correspondence to: lbd2126@columbia.edu (L.B.D.)
Present address: Atai Life Sciences, New York NY 10012, USA (T.K.)

Abstract

Female *Aedes aegypti* mosquitoes can spread disease-causing pathogens when they bite humans to obtain blood nutrients required for egg production. Following a complete blood meal, host-seeking is suppressed until eggs are laid. Neuropeptide Y-like Receptor 7 (NPYLR7) plays a role in endogenous host-seeking suppression and previous work identified small molecule NPYLR7 agonists that suppress host-seeking and blood feeding when fed to mosquitoes at high micromolar doses. Using structure activity relationship analysis and structure-guided design we synthesized 128 compounds with similarity to known NPYLR7 agonists. Although *in vitro* potency (EC_{50}) was not strictly predictive of *in vivo* effect, we identified 3 compounds that suppressed blood feeding from a live host when fed to mosquitoes at a 1 μM dose, a 100-fold improvement over the original reference compound. Exogenous activation of NPYLR7 represents an innovative vector control strategy to block mosquito biting behavior and prevent mosquito/human host interactions that lead to pathogen transmission.

Introduction

Female *Aedes aegypti* mosquitoes are innately attracted to find and bite human hosts to obtain blood protein required for egg development. However, host-seeking behavior is regulated by the female's internal state and is naturally suppressed after a full meal of blood, during egg development (Judson CL, 1967). Blood nutrients are required for sustained suppression; although female mosquitoes will engorge on non-nutritive saline meals that cannot support egg development these females return to high levels of host-seeking when abdominal distensions wears off roughly 24 hours later (Duvall et al., 2019; Galun, 1963; Klowden and Lea, 1979b). Previous work implicates abdominal mechanosensors in mediating short-term suppression and neuropeptide pathways in mediating sustained, days-long, suppression (Brown et al., 1994; Christ et al., 2018; Davis, 1984; Duvall et al., 2019; Klowden, 1981; Klowden and Lea, 1979a, 1979b; Liesch et al., 2013). Neuropeptide Y-related pathways regulate hunger and satiety in many organisms (Colmers and Wahlestedt, 1993; De Bono and Bargmann, 1998; Inui, 1999; Kuenzel et al., 1987; Wu et al., 2003) and we recently identified *Aedes aegypti* Neuropeptide Y-like Receptor 7 (NPYLR7) as a key regulator of host-seeking after a blood meal (Duvall et al., 2019). After blood feeding, NPYLR7 activation acts as a satiety signal and suppresses attraction to hosts. Pharmacological activation of NPYLR7 inhibits biting and blood feeding even in the absence of blood nutrients. Conversely, female mosquitoes with genetically or pharmacologically disrupted NPYLR7 signaling continue to host-seek inappropriately after a blood meal. Exogenous activation of feeding-related neuropeptide receptors in mosquitoes represents a novel approach to block their attraction to humans by exploiting the pathways that naturally suppress the drive to bite.

Here, we used structure activity relationship analysis and structure-guided design to identify novel small molecule NPYLR7 agonists with improved *in vitro* and *in vivo* potency compared to compounds identified in a previous high-throughput small molecule screen of 265,211 compounds (Duvall et al., 2019). We synthesized 128 new compounds and characterized their *in vitro* potency using an HEK cell-based assay to evaluate NPYLR7 activation. To identify those with *in vivo* activity, we tested 30 compounds in a host-seeking screening assay and subsequently identified 3 compounds that significantly reduced blood feeding from a live host

66 when delivered to mosquitoes at a 1 μM, a dose 100-fold lower than that used in our original
67 report (Duvall et al., 2019).
68
69 Although 3 out of 30 compounds tested *in vivo* suppressed host-seeking behavior, *in vitro*
70 potency was not highly predictive of *in vivo* efficacy. This disconnect highlights the need for
71 intermediate assays to span the gap between cell-based and behavioral assays in mosquitoes.
72 This work is important because it identifies new highly potent compounds that block mosquito
73 blood feeding by targeting a neuropeptide receptor that regulates mosquito attraction to
74 humans through a conserved satiety pathway.

Results

We previously showed that pharmacological activation of NPYLR7 suppressed *Aedes aegypti* mosquito host-seeking when delivered in a non-nutritive saline meal and we identified small molecule NPYLR7 agonists that induce host-seeking suppression independent of nutrient consumption (Figure 1A). However, the most potent of these compounds (TDI-012631) had a half-maximal effective concentration (EC_{50}) in activating NPYLR7 *in vitro* of 19.6 μM and was behaviorally active only when fed at high micromolar doses (> 30 μM). We therefore set out to design and evaluate analogs of this compound to identify those with improved potency. We generated a docking model of TDI-012631 bound to NPYLR7 to identify protein-ligand interactions that could inform analog design. The docking model showed that the quinazoline core occupies a hydrophobic pocket in the orthosteric binding site formed by transmembrane helices 3, 5, and 6. The guanidine substituent is stabilized by a salt bridge interaction with the Glu198 side chain in EL2 loop, while the 4-position methyl group is pointed toward $Gln122^{3.32}$ and 7-position methoxy group is oriented toward $Phe218^{5.47}$ (Figure 1B). This docking model is in agreement with early structure-activity relationship data for close analogs of TDI-012631, where the quinazoline core and guanidine appear to form a minimum pharmacophore. Indeed, replacement of the guanidine group with an amine (compound TDI-012610) causes a loss of potency. Newly synthesized analogs were then tested using a calcium-based HEK293T assay to determine their *in vitro* potency compared to FMRFa3, an endogenous peptide ligand of NPYLR7 (Figure 1 C and D). We used the original reference compound, TDI-012631, as a benchmark for potency. Based on the *in vitro* assay, compounds were grouped by EC_{50} value into those that showed low sensitivity or potency (> 100 μM), those with *in vitro* EC_{50} values < 100 μM but > 4.11 μM (TDI-012631, reference compound) and those with EC_{50} values < 4.11 μM.

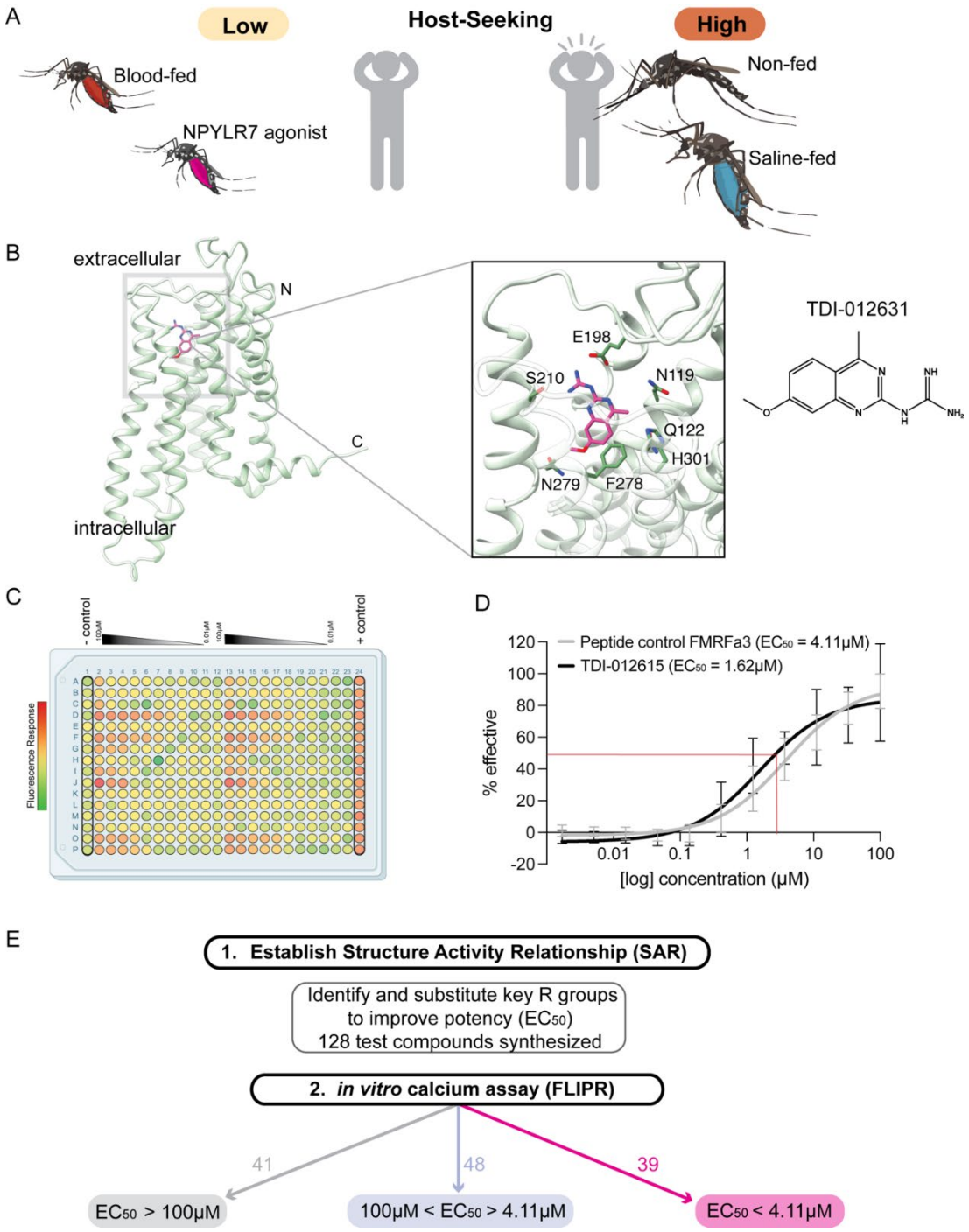

Figure 1: Structure-guided design to synthesize novel NPYLR7 agonists
(A) Representation of *Aedes aegypti* host-seeking behavior by feeding status. (B) NPYLR7 predicted structure model with compound TDI-012631 bound (left) and predicted side chain interactions (right). (C) Representative 384 well plate layout from *in vitro* screen displaying Raw Fluorescent Units (RFU) corresponding to test compounds ranging from concentration of 100 - 0 μM from left to right. Negative control (column 1) is measured as response to assay buffer alone and positive control (column 24) is response to 10 μM dose of FMRFa3, an endogenous peptide activator of NPYLR7. (D) Semilogarithmic curves of compound TDI-012615 (EC_{50} = 1.62 μM, black line) and FMRFa3 (peptide control) sigmoidal curve (EC_{50} = 4.11 μM, gray line). (E) Outline of *in vitro* screening for 128 newly synthesized NPYLR7 agonists binned according to *in vitro* EC_{50}.

111 Analogs of TDI-012631 were designed by maintaining the quinazoline core and the guanidine
112 substituent that formed critical interactions in the docking model and modifying the substituents
113 around the core at the 4 (R2), 6 (R1), and 7 (R) positions (Figure 2A). Bulkier groups were
114 explored for R to extend into the deeper pocket, while hydrogen-bond donating $NHCH_3$ group
115 was introduced for R2 to interact with Gln122$^{3.32}$ side chain (Figure 2A). Over a hundred
116 compounds were designed and synthesized. To identify compounds with *in vivo* activity, thirty
117 compounds were selected for testing in host-seeking assays. This group included compounds
118 with predicted EC_{50} values ranging from 39.3 μM to 1.92 nM as well as a negative control
119 compound from the > 100 μM group (Figure 2B).
120
121 To prioritize candidates with highest levels of *in vivo* efficacy we performed a screening
122 "Miniport olfactometer" assay that allowed us to test mosquito host-seeking behavior in 4
123 conditions in parallel (Figure 3A). In this assay we provided two host cues, CO_2 and human
124 odor collected on a worn nylon stocking. Animals were scored as attracted if they flew from the
125 starting canister into the attraction trap next to the source of the host cues. Animals were fed
126 each compound at a 1 μM dose in non-nutritive saline 2 days prior to testing, then scored and
127 weighed to ensure that compounds did not affect meal palatability or consumption (Data S1).
128 Animals were allowed to recover for 2 days before host-seeking assays were performed to
129 ensure that suppression was not attributable to abdominal distension from meal consumption.
130 Using the Miniport olfactometer assay we identified compounds that suppressed host-seeking
131 compared to saline alone (Figure 3B). Consistent with previous work, the original lead
132 compound TDI-012631, was not active at a 1 μM dose. We plotted the relationship between *in*
133 *vitro* EC_{50} and *in vivo* efficacy in the Miniport assay and found that, although we identified
134 compounds that were more effective than TDI-012631 there was no predictive relationship
135 between *in vitro* EC_{50} and *in vivo* efficacy (Figure 3C).
136
137 We next asked whether compounds that suppressed attraction to host cues in the Miniport
138 olfactometer assay could also block blood feeding from a live host using a "Mouse in Cage"
139 assay in which mosquitoes are fed test compounds and presented with an opportunity to blood
140 feed from an anesthetized mouse 2 days later. Non blood-fed females were robustly attracted
141 to the mouse and blood fed at high rates (91.0 ± 1.92%), while females that were naturally

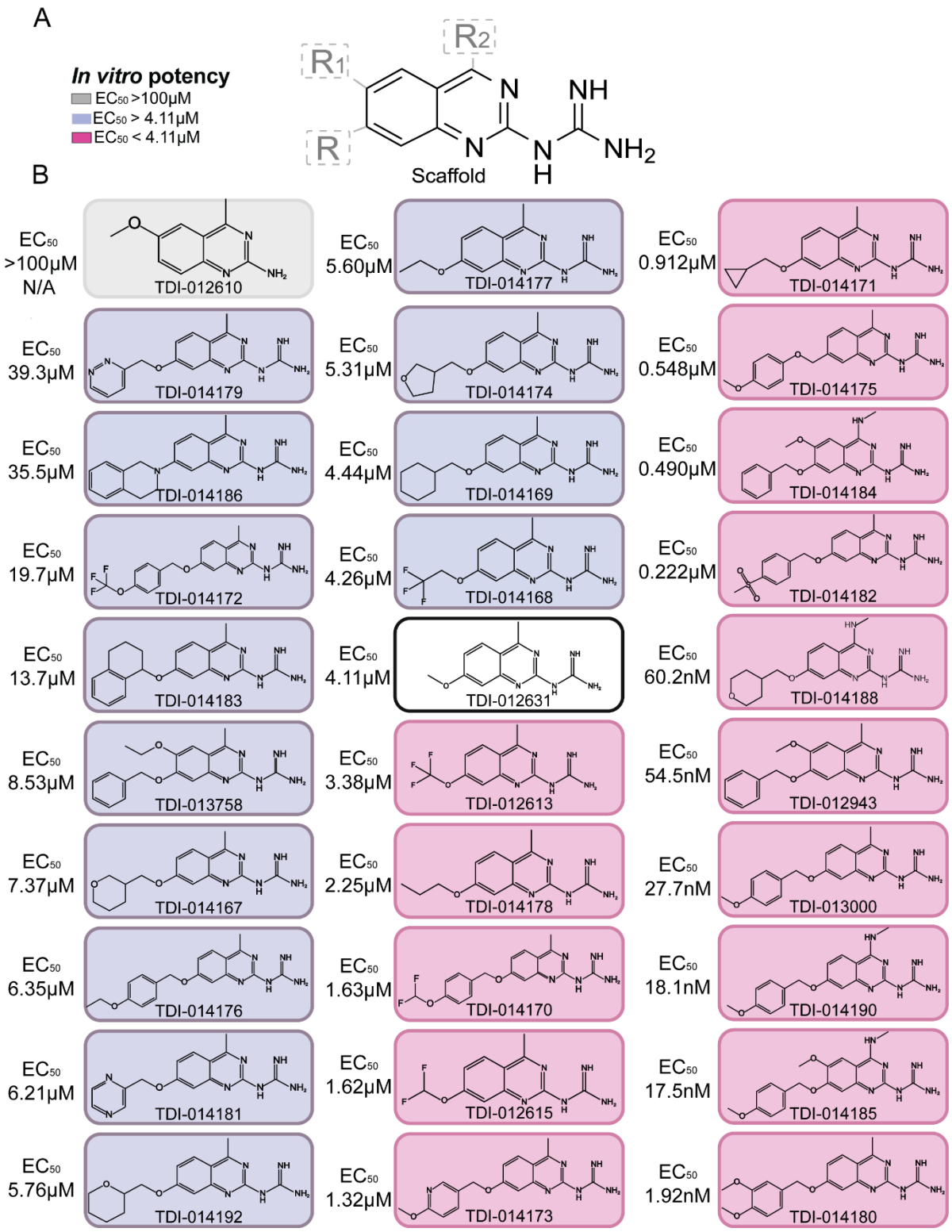

Figure 2: Small molecule NPYLR7 agonists tested *in vivo*
(A) Lead compound scaffold with conserved quinazoline core and R groups tested for substitutions. Shading in legend indicates EC_{50} in (B). (B) Chemical structures with corresponding *in vitro* EC_{50} of each compound tested in behavioral assays arranged with the highest value at the top left to the lowest value at bottom right. TDI-012631 (center, black border) is the initial reference compound.

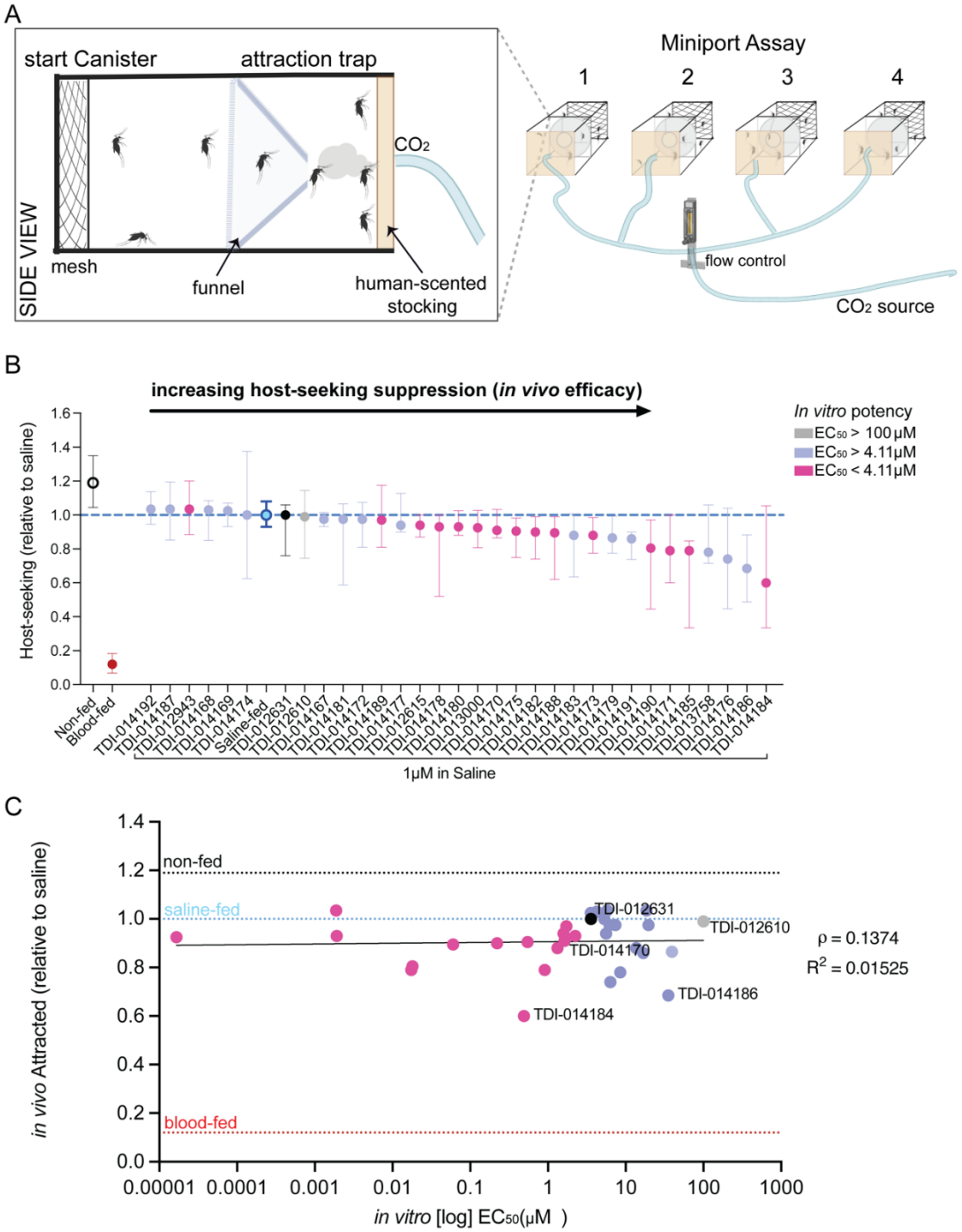

Figure 3: Miniport olfactometer screening assay to identify compounds that suppress attraction to human host cues

(A) Schematic of Miniport Olfactometer host-seeking assay. Inset depicts start canister and attraction trap modular components for each experiment. Mosquitoes not drawn to scale. (B) Host-seeking suppression relative to saline (test compound % host seeking/ average matched saline % host-seeking). (Median with interquartile range, n = 4 – 65 replicates, 15-20 females/replicate). (C) Correlation of *in vitro* potency to *in vivo* host seeking suppression in *Aedes aegypti*. Spearman correlation coefficient (ρ) = 0.1374, $p > 0.05$, slope = 0.002942, R^2 = 0.01525.

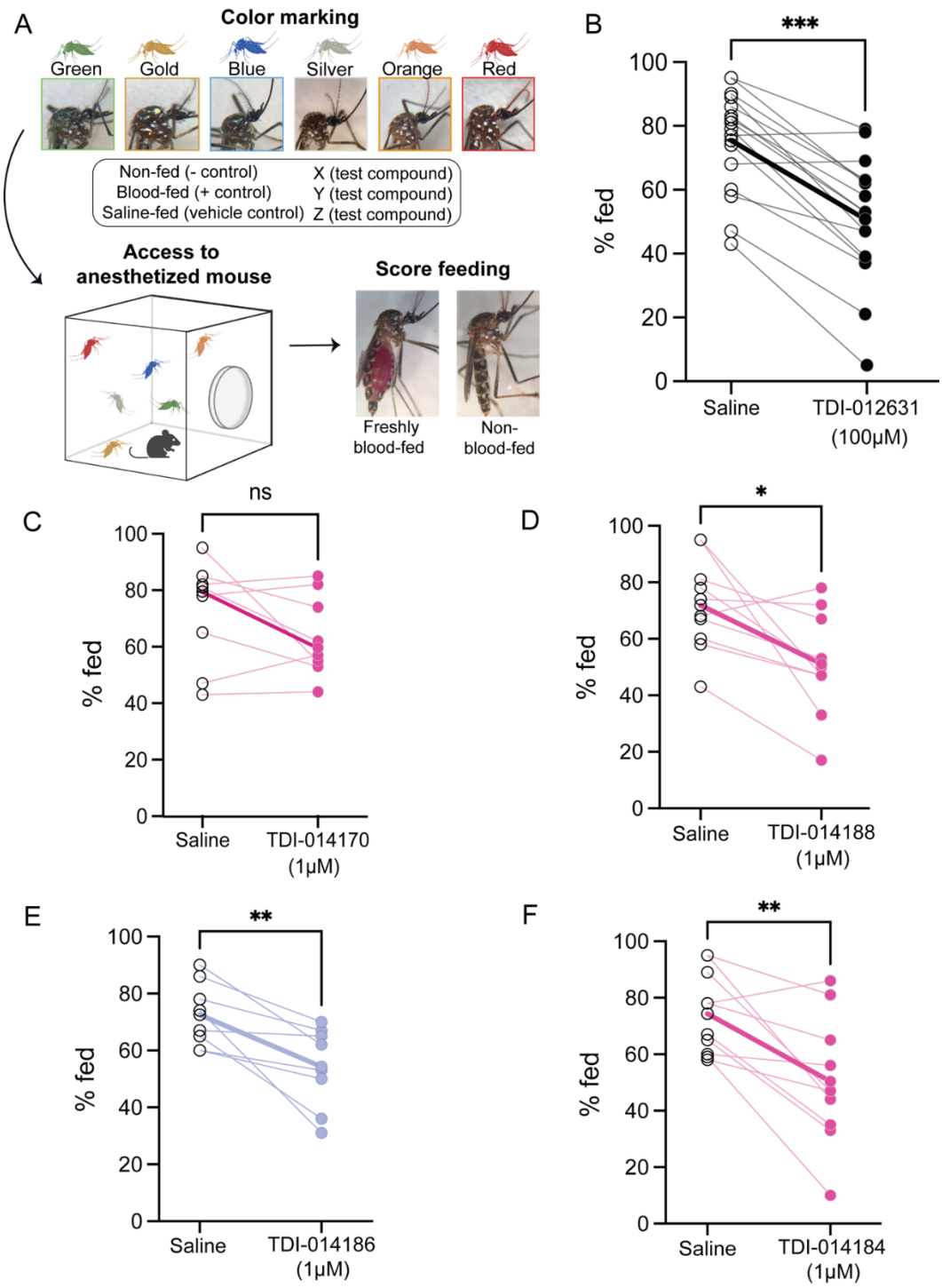

Figure 4: Novel NPYLR7 agonists suppress blood feeding from a live host when fed at 1 μM dose
(A)Schematic of "mouse in cage" biting assay workflow depicting powder color assignment, exposure to mouse, and scoring of fresh blood in the abdomen. (B – F) Percentage of females that freshly blood fed on an anesthetized mouse after 15 minute exposure. Females were fed the indicated meal 48 hours prior to the experiment. (C,D,F) are high potency and (E) is a medium potency *in vitro* compound (See Figure 2B). Bold lines represent saline group mean compared to test group mean. 15 – 20 females per replicate. Mann-Whitney test: (B) n = 13 replicates, ***p = 0.0003, (C) n= 9 replicates, ns, not significant, p = 0.2868, (D) n= 11 replicates, *p = 0.0120). (E) n= 9 replicates, ** p = 0.0097, (F) n= 11 replicates; ** p = 0.0055.

169 suppressed after a meal of sheep blood rarely fed (7.0 ± 1.21%) (Data S1). At the end of each
170 experiment mosquitoes were collected and scored for the presence of fresh blood in their
171 abdomen, indicating that they successfully fed on the blood of the mouse (Figure 4A). We
172 replicated the finding that TDI-012631 suppressed blood feeding when fed to mosquitoes at a
173 100 μM dose (Figure 4B) (Duvall et al., 2019). Although TDI-014170 showed high *in vitro*
174 potency (EC_{50} = 1.63 μM), this compound did not reduce host-seeking in our Miniport
175 olfactometer screening assay nor did it significantly reduce biting in the Mouse in Cage assay
176 when fed at a 1 μM dose (Figure 4C). However, we identified 3 novel small molecule NPYLR7
177 agonists that reduced biting behavior when fed at a 1 μM dose (Figure 4 D – F). These
178 included TDI-014188 and TDI-014186, which were the 2 compounds that showed the largest
179 effect in the Miniport host-seeking assay (Figure 3B). Although two of the three active
180 compounds TDI-014184 (EC_{50} = 0.490 μM) (Figure 4F) and TDI-014188 (EC_{50} = 60.2 nM)
181 (Figure 4D) showed significantly improved *in vitro* potency compared to the reference
182 compound, surprisingly, (TDI-014186) (Figure 4E) effectively suppressed biting despite
183 showing lower *in vitro* potency (EC_{50} = 35.5 μM) compared to the reference compound.

Discussion

Multiple mosquito genera contribute to the spread of human disease. *Aedes* mosquitoes can transmit the dangerous arboviruses yellow fever, dengue, Zika, and chikungunya (Bhatt et al., 2013; Weaver et al., 2013). The emergence and geographical spread of these viruses are critical concerns for global public health (Bhatt et al., 2013; Kraemer et al., 2015; Ryan et al., 2019). Although much research has been dedicated to developing vaccines and prophylactic or therapeutic drugs to treat and prevent these diseases there are currently no drugs to treat the viruses spread by *Aedes aegypti.* Although there is an effective vaccine against the yellow fever virus and there have been significant improvements in recent dengue vaccination strategies (Adams et al., 2021), preventing mosquito bites remains essential for reducing disease transmission. Current strategies to control mosquito populations rely on toxic pesticides that decline in efficacy as mosquito populations rapidly develop resistance (Moyes et al., 2021). More recently-developed approaches involve the release of mosquitoes rendered either sterile or unable to transmit pathogens (Blumberg et al., 2016; Lees et al., 2015) or releasing transgenic animals with altered immune or reproductive function (Hammond et al., 2016; Macias et al., 2017; Parihar et al., 2020). However, ethical, environmental, and regulatory concerns remain issues in deployment of such transgenic mosquitoes. Although each of these approaches has shown some success, there remains major unmet need to develop innovative and complementary strategies for integrated mosquito control.

The most prevalent chemical control methods include synthetic insecticides or repellents and previous studies have primarily focused on determining pharmacokinetic properties of these compounds in non-target vertebrates at doses lethal to the target insect (González-Morales et al., 2023; Qiu et al., 1997). Lethality contributes to evolution of resistance by selecting for individuals carrying resistance alleles that can escape lethality (Liu, 2015; Su et al., 2019). Most insecticides are limited to a few chemical classes with similar mechanisms of action and the World Health Organization has urged the development of new mosquito control techniques that exploit novel chemical classes (World Health Organization, 2012). Increasingly, new strategies have focused on non-lethal methods of pest control (Savino et al., 2018; Witmer et al., 2017). This category includes the small molecule NPYLR7 agonists tested in this study,

215 which reduce the drive to bite without killing the mosquito. However, there is a need for
216 relevant drug discovery assays in insects to characterize the utility and potential for
217 development of non-lethal chemicals. In traditional drug discovery and development, *in vitro*
218 assays to determine potency are normally followed by assays to determine target engagement
219 in cells and pharmacokinetic/pharmacodynamic (PK/PD) properties to evaluate how
220 compounds are absorbed, metabolized and eliminated from specific tissues in the body. There
221 are examples of insect models for drug discovery; silkworms (*Bombyx mori*) have been used
222 as a model for drug toxicity and show responses to hepatotoxic drugs that are consistent with
223 mammalian models (Hamamoto et al., 2009; He et al., 2020). More recent work has
224 established novel models for pharmacokinetic assays in mosquitoes by delivering ivermectin
225 and cytochrome P450 modulators in blood, using liquid chromatography with tandem mass
226 spectrometry (LC-MS/MS) to quantify clearance rates after feeding, and modeling primary
227 pharmacokinetic parameters and drug/drug interactions. Ivermectin clearance kinetics differ
228 between mosquitoes compared to mammals, and individual P450 modulators were eliminated
229 with differing kinetics in mosquitoes (Duthaler et al., 2021). However, detection remains a
230 limiting factor. Drug concentrations are higher than those that can be obtained in the blood of
231 humans receiving a regular dose of ivermectin and because whole mosquito specimens were
232 required for analysis it is not yet possible to achieve tissue-specific resolution of drug
233 occupancy/clearance. We found that *in vitro* EC_{50} was not predictive of behavioral effect
234 among the compounds tested in our assays and future work to characterize the clearance
235 rates of the compounds described here may clarify the relationship between EC_{50} in our cell-
236 based assay and behavioral effect. Compounds like TDI-014170 with high *in vitro* potency may
237 be inactive *in vivo* because they lack bioavailability in the mosquito, or have a half-life that is
238 too short to be captured when assays are performed 2 days after feeding. Compounds like
239 TDI-014186 that suppressed host-seeking behavior despite modest *in vitro* EC_{50} may achieve
240 *in vivo* potency through sequestration in specific target tissues.
241
242 NPY-like receptors are present in many insects including other blood-feeding arthropods
243 (Garczynski et al., 2005; Gulia-Nuss et al., 2016). This suggests that NPY pathways may
244 represent a conserved biological mechanism that could be targeted for the development of a
245 more generalized strategy to suppress attraction to humans across multiple species of

mosquitoes and ticks. To ensure that beneficial insects are not impacted, *in vitro* assays to identify compounds that show minimal cross-activation of related receptors in other insect species will be crucial. Delivering these compounds in traps baited with human odor will also ensure that beneficial insects are not targeted, a method is already in use in attractive toxic sugar baits (Fiorenzano et al., 2017; Krockel et al., 2006; Mukabana et al., 2012; Okumu et al., 2010).

By combining advanced molecular modelling, medicinal chemistry and precise deployment strategies, there is potential to develop targeted and environmentally responsible solutions for managing mosquito populations. Continued research into the structural aspects of these compounds and their receptor interactions will pave the way for the development of next-generation insect control agents with broader applicability and improved efficacy. Further study of the structural relationship between these compounds and *Aedes aegypti* NPYLR7 may help to identify new highly potent compounds and the rules by which they activate their cognate receptors.

Acknowledgements

We thank Gloria Gordon, Libby Mejia, and Ellen de Obaldia for assistance with mosquito rearing and Jim Petrillo for support with Miniport construction. Support for this project was provided by an Advanced Grant from the Robertson Therapeutic Development Fund, generously provided by the Robertson Foundation. The authors gratefully acknowledge the support to the project generously provided by the Sanders Tri-Institutional Therapeutics Discovery Institute (TDI), a 501(c)(3) organization. TDI receives financial support from Takeda Pharmaceutical Company, TDI's parent institutes (Memorial Sloan Kettering Cancer Center, The Rockefeller University and Weill Cornell Medicine) and from a generous contribution from Mr. Lewis Sanders and other philanthropic sources. This work was partially supported by a Clinical and Translational Science Award (UL1 TR001866) from the National Center for Advancing Translational Sciences at the National Institutes of Health to C.S.J., a grant from NIGMS (R35 GM137888), a Beckman Young Investigator Award, a Pew Scholar in Biomedical Sciences Award, and a Klingenstein-Simons Fellowship Award in Neuroscience to L.B.D. L.B.V. is supported by the Howard Hughes Medical Institute.

Author Contributions

Mayako Michino and D.H. carried out molecular modeling, T.K. and Mike Miller coordinated compound synthesis, and L.A.B. coordinated compound profiling and *in vitro* data analysis. C.S.J. provided statistical expertise for *in vivo* data analysis. E.V.Z. carried out all *in vivo* experiments. E.V.Z., L.B.D., and L.B.V. conceived the study, designed the figures, and wrote the paper, with input from all authors.

Materials and Methods

Molecular modelling for the NPYLR7 agonist series

The docking model for the NPYLR7 agonist series was generated based on a homology model of *Aedes aegypti* NPYLR7 and validated with rigorous FEP+ binding energy calculations (Abel et al., 2017). The homology model of *Aedes aegypti* NPYLR7 was obtained from the GPCR-I-Tasser homology modeling server (https://zhanggroup.org/GPCR-I-TASSER/) (Zhang et al., 2015). To predict the binding mode of reference compound TDI-012631, the compound was docked to the orthosteric binding site of NPYLR7 homology model using Glide SP, then the receptor-ligand complex was refined in a POPC lipid bilayer environment using Desmond molecular dynamics (MD) simulation for 120 ns at constant temperature of 300K in NPγT ensemble. The protein structure was prepared using the Protein Preparation Wizard in Maestro with default settings. The ligand structure was prepared using LigPrep in Maestro. The protonated form of the ligand was selected, according to the predicted pKa of the guanidine moiety (pKa = 10.21 in Jaguar). The MD simulations were carried out using the OPLS3e force field (Harder et al., 2016). The final snapshot at 120 ns was minimized and then subjected to an absolute FEP+ calculation, (Khalak et al., 2021) which showed favorable binding energy ($\Delta G = -18.02 \pm 0.24$ kcal/mol). To further validate the docking model, relative FEP+ calculations were performed on a validation set of 13 compounds in the series having EC_{50} values ranging across 3 log units. The validation showed good agreement between the experimental and FEP+ predicted potencies (MUE = 1.29 kcal/mol; $R^2 = 0.57$). The perturbation maps were automatically generated using the Mapper tool. Force Field Builder was employed to generate custom torsional parameters for ligand torsions that were not include in the default force field. FEP+ calculations were run for the default 5 ns. The Schrödinger Suite was used for protein and ligand preparations, docking, MD, and FEP+ calculations (release 2020-4, Maestro, Schrödinger LLC, New York, NY).

Synthetic methods for analog preparation

Unless otherwise noted, the following pertain to the synthetic methods: all reactions are magnetically stirred; typical solvents (ethyl acetate, hexanes, dichloromethane, and methanol) are Fisher Optima grade; “concentrated to dryness” or “removal of the solvent” means evaporating the solvent from a solution or mixture using a rotary evaporator; flash chromatography is carried out on an Isco, Analogix, or Biotage automated chromatography system using a commercially available cartridge as the column. Columns are usually filled with silica gel as the stationary phase; preparative HPLC (or prep-HPLC) is carried out with commercial columns in a reverse phase manner (the stationary phase is hydrophobic). Typical solvent mixtures include A (water) and B (organic i.e. acetonitrile, methanol, etc.). Additives can also be used in the solvent mixture such as HCl, NH_4HCO_3, and formic acid. Details for individual synthesis reactions are provided in Supplemental Methods.

In vitro Assay

The *in vitro* screening assay was adapted from (Duvall et al., 2019), and carried out at HD Biosciences (HDB, Shanghai) as follows: HEK293T (ThermoFisher Scientific) cells were grown in DMEM (high glucose, with glutamine), 10% Fetal Bovine Serum, 1% Pen/Strep, seeded in a 75 cm^2 flask, and incubated at 37°C and 5% CO_2. Cells were transiently transfected with 1 μg of each plasmid expressing GCaMP6s (Addgene #277314.1040753) (Chen et al., 2013),

329 mouse Gqα15 (Addgene #40753) (Offermanns and Simon, 1995) and *Aedes aegypti* NPYLR7
330 (Addgene #52392) (Duvall et al., 2019) using Lipofectamine 2000 (Invitrogen) in 4mL of Opti-
331 Mem (Invitrogen). This mixture was added to a plate after 20 minutes and incubated for 6 - 8
332 hours. Cells were then trypsinized, resuspended in phenol-free media, and plated in a 384 well
333 plate (Greiner Bio-one) at a density of 20,000 cells per 40 μL, and incubated overnight (37°C,
334 5% CO_2). Cells were imaged directly in phenol-free mediate. Plates were loaded into a
335 Molecular Devices Fluorescent Imaging Plate Reader (FLIPR) with an excitation wavelength of
336 470 – 495 nm and an emitted wavelength of 515 – 575 nm. Plates were imaged every second
337 for 5 minutes. After 30 seconds of baseline fluorescence recording, 10 μL of test compound in
338 Reading Buffer ([Hanks's Balanced Salt Solution (GIBCO) + 20 mM HEPES (Sigma-Aldrich)]
339 was added. Concentrations tested ranged from 0 - 100 μM. Data was collected in raw
340 fluorescence units (RFU).
341

342 ## EC_{50} Calculations

343 Each test plate included replicates of 10 μM FMRFa3, an *Aedes aegypti* neuropeptide agonist
344 of NPYLR7 used to calculate Hundred Percent Effect (HPE). The Zero Percent Effect (ZPE)
345 control was calculated as response to buffer alone. Z' Factor was calculated for each plate by
346 $Z' = 1 - \frac{3\sigma_{HPE}+3\sigma_{ZPE}}{|\mu_{HPE-}\ \mu_{ZPE}|}$. Plates with Z' < 0.5 were excluded from analysis. Raw Fluorescent Units
347 (RFUs) were converted to percent effect relative to the average of the ZPE and HPE. Percent
348 Effect = (sample luminescence-average ZPE)/(average HPE-average ZPE)*100. Doses
349 ranged from 0 to 100 μM, the highest 100 μM dose was excluded in replicates in which this
350 dose showed aberrant responses beyond plateau (defined as 2 points with < 15% change).
351 Each replicate was plotted as percent effect vs log[concentration] and replicates with maximal
352 responses between 20% and 250% were used for EC_{50} calculations. Relative EC_{50} was
353 calculated using a [Agonist] versus response - variable slope four parameter model where $Y =$
354 $Bottom + \frac{(X^{Hillslope})*(Top-Bottom)}{(X^{HillSlope}+EC50^{HillSlope})}$. For compounds with multiple replicates, the relative EC_{50} of
355 each replicate was averaged.
356

357 ## Mosquito Rearing and Maintenance

358 *Aedes aegypti* (Orlando strain) were reared and maintained in a STERIS environmental room
359 under the following conditions: 26 - 28°C, 80% humidity. Light cycles consisted of 14:10 hr
360 (L:D). Eggs were hatched in hatching broth: 1 fish food tablet (TetraMin Tropical Tablets, Pet
361 Mountain) crushed using a mortar and pestle brought to a volume of 850 mL diH2O and
362 autoclaved for sterility). During larval stages (days 2 - 5), larvae were fed 2 tablets of fish food
363 per day. Pupae were collected and allowed to eclose in 91 cm × 61 cm × 61 cm BugDorm
364 cages (BioQuip Products). Adults were provided with cotton dental wicks (Richmond Dental)
365 inserted into Boston clear round 60 mL glass bottle (ThermoFisher) filled with 10% sucrose
366 (w/v). Adults were co-housed with siblings and allowed to mate freely for seven days post-
367 eclosion. All behavioral experiments were performed using 14 - 21-day old females as in
368 (Duvall et al., 2019). Males were removed prior to all behavioral experiments.
369

370 ## Glytube feeding

371 Groups of 60 - 150 females were placed in 21.6 cm diameter x 16.5 cm height bucket cages
372 (VWR) and fasted with access to water for 24 hours prior to feeding. Meals were delivered to

373 females via Glytube membrane feeders as described (Costa-da-Silva et al., 2013). Meals
374 consisted of 1.5 mL sheep blood (Hemostat Laboratories), saline (400 mM $NaHCO_3$ + dih_2O),
375 or saline and test compound. Lyophilized compounds were stored at room temperatures until
376 use. High concentration stocks (30 mM in 100% DMSO) (Sigma-Aldrich) were stored at -20°C
377 and diluted in saline immediately prior to feeding. Once prepared, meals and glycerol heating
378 elements were warmed in a 42°C water bath for 15 minutes to provide warmth to attract
379 mosquitos to feed. ATP (1 mM final concentration) and test compounds (1 μM final
380 concentration) were added prior to placing the meal on top of the mesh on the cage containing
381 female mosquitos. Females were allowed 15 - 20 minutes to feed to repletion. Abdominal
382 engorgement was scored by eye and confirmed by weighing females to ensure full feeding
383 (Data S1). Females that did not feed to repletion were discarded. Females were returned to
384 their original cage with a diH_2O wick for 48 hours prior to behavioral testing. Lethality of each
385 compound was measured by counting the number of dead females in each cage 24 hours post
386 meal. Any compounds that resulted in > 50% death rate were scored as "high lethality" and
387 excluded from behavioral testing.
388

389 ## Behavior

390 ### Host Seeking Screening Assay (Miniport Olfactometer)

391 Miniport olfactometers were fabricated in-house as described (Duvall et al., 2019). Information
392 regarding design, construction, and use can be found at
393 https://github.com/VosshallLab/Miniport-Construction. Miniport canisters consisted of a 6'' x 3''
394 x 3'' acrylic tube with a mesh screen to allow for air flow. Groups of 10 - 20 females were
395 loaded into canisters 24 hours post meal. Females were left in canisters overnight to acclimate
396 with two cotton balls soaked in diH_20 to prevent desiccation. Behavior trials began 48 hours
397 post meal. Canisters were randomly assigned to attraction traps 1 - 4 and given 5 minutes to
398 acclimate. The stimulus end of the trap was connected to a flowmeter that supplied 5% CO_2 at
399 a rate of 30 mL/min. Thirty seconds of CO_2 flow was supplied to activate females prior to
400 opening the sliding door. Once opened, the sliding door gave females access to the attraction
401 trap baited with a human scented nylon stocking previously worn by the same experimenter for
402 8 -10 hours to collect body odor and stored in a plastic bag at -20°C until use. After 5 minutes,
403 the sliding door was closed and attraction was scored as mosquitoes in attraction trap/total
404 number mosquitoes. For each experiment data were normalized to the matched average
405 saline attraction from the same experiment (% attracted/average saline attraction). Any dead
406 mosquitoes were excluded from analysis. Non-fed females and blood-fed females served as
407 environmental control groups while the saline-fed females served as the vehicle control each
408 day. If non-fed or saline-fed females were less than 50% attracted or if blood-fed females were
409 more than 20% attracted behavioral trials were halted and all data from that experimental day
410 were discarded.
411

412 ### Biting Assay (Mouse in cage)

413 This assay was modified from (Duvall et al., 2019). Females were fed and scored as described
414 above. 48 hours post meal, females were anesthetized in a 4°C cold room and aspirated into a
415 petri dish (ThermoFisher Biosciences) with a randomly assigned color powder (Slice of the
416 Moon; Chameleon Colors) to mark their treatment group. Females were then individually
417 removed from the color powder, placed inside a 91 cm × 61 cm × 61 cm cage (BugDorm), and
418 allowed 2 - 4 hours to recover. Each experiment consisted of a cage with 12 - 20 females in

each treatment group including environmental (non-fed and blood-fed) and vehicle (saline-fed) control groups. The experiment began once an anesthetized mouse was introduced to the center of the cage and females were allowed 15 minutes to blood feed. The mouse was then removed, and the cage was placed at 4°C to anesthetize females for collection. Females were aspirated into a large glass petri dish (Pyrex) and scored under a dissection microscope for powder color and blood feeding status (Nikon SMZ1500). Females were scored as “blood-fed” if fresh blood was present in the abdomen. Percent biting was calculated as females freshly blood fed/total females in each respective treatment group.

Quantification and statistical analysis

All statistical analysis was performed using GraphPad Prism Version 10. Data collected as percentage of total are shown as median with range. Data collected as raw values are shown as mean ± SEM or mean ± SD. Details of statistical methods are reported in the figure legends.

Data and software availability

Raw data are provided in Data S1. Cartoons in Figures 1, 3, and 4 were created with BioRender.com. Chemical structures in Figures 1 and 2 were generated with ChemDraw (version 21.0.0). The Schrödinger Suite was used for protein and ligand preparations, docking, MD, and FEP+ calculations (release 2020-4, Maestro, Schrödinger LLC, New York, NY).

Human and animal ethics statement

Blood-feeding procedures and mosquito behavior with human scent collected on nylon were approved and monitored by The Rockefeller University Institutional Review Board (IRB protocol LVO-0652) and the Rockefeller University Institutional Animal Care and Use Committee (IACUC protocol 20068-H). Human subjects gave their written informed consent to participate in this study.

446 # References
447
448 Abel R, Wang L, Harder ED, Berne BJ, Friesner RA. 2017. Advancing Drug Discovery through
449 Enhanced Free Energy Calculations. *Acc Chem Res* **50**:1625–1632.
450 doi:10.1021/acs.accounts.7b00083
451 Adams LE, Waterman S, Paz-Bailey G. 2021. Vaccination for Dengue Prevention. *JAMA*
452 **327**:817–818. doi:10.1001/jama.2021.23466
453 Bhatt S, Gething PW, Brady OJ, Messina JP, Farlow AW, Moyes CL, Drake JM, Brownstein
454 JS, Hoen AG, Sankoh O, Myers MF, George DB, Jaenisch T, Wint GRW, Simmons CP,
455 Scott TW, Farrar JJ, Hay SI, William Wint GR, Simmons CP, Scott TW, Farrar JJ, Hay SI,
456 Wint GRW, Simmons CP, Scott TW, Farrar JJ, Hay SI. 2013. The Global Distribution and
457 Burden of Dengue. *Nature* **496**:504–507. doi:10.1038/nature12060
458 Blumberg BJ, Short SM, Dimopoulos G. 2016. Employing the Mosquito Microflora for Disease
459 Control, Genetic Control of Malaria and Dengue. Elsevier Inc. doi:10.1016/B978-0-12-
460 800246-9.00015-6
461 Brown MR, Klowden MJ, Crim JW, Young L, Shrouder LA, Lea AO. 1994. Endogenous
462 Regulation of Mosquito Host-seeking Behavior by a Neuropeptide. *J Insect Physiol*
463 **40**:399–406. doi:10.1016/0022-1910(94)90158-9
464 Christ P, Hill SR, Schachtner J, Hauser F, Ignell R. 2018. Functional characterization of
465 mosquito short neuropeptide F receptors. *Peptides* **103**:31–39.
466 doi:10.1016/j.peptides.2018.03.009
467 Colmers WF, Wahlestedt C. 1993. The Biology of Neuropeptide Y and related peptides.
468 Springer Science & Business Media.
469 Costa-da-Silva AL, Navarrete FR, Salvador FS, Karina-Costa M, Ioshino RS, Azevedo DS,
470 Rocha DR, Romano CM, Capurro ML. 2013. Glytube: A Conical Tube and Parafilm M-
471 Based Method as a Simplified Device to Artificially Blood-Feed the Dengue Vector
472 Mosquito, Aedes aegypti. *PLoS One* **8**:e53816. doi:10.1371/journal.pone.0053816
473 Davis EE. 1984. Regulation of sensitivity in the peripheral chemoreceptor systems for host-
474 seeking behavior by a haemolymph-borne factor in Aedes aegypti. *J Insect Physiol*
475 **30**:179–183. doi:10.1016/0022-1910(84)90124-0.
476 De Bono M, Bargmann CI. 1998. Natural variation in a neuropeptide Y receptor homolog
477 modifies social behavior and food response in C. elegans. *Cell* **94**:679–689.
478 doi:10.1016/S0092-8674(00)81609-8
479 Duthaler U, Weber M, Hofer L, Chaccour C, Maia M, Müller P, Kraähenbuähl S, Hammann F.
480 2021. The pharmacokinetics and drug-drug interactions of ivermectin in Aedes aegypti
481 mosquitoes. *PLoS Pathog* **17**:1–18. doi:10.1371/journal.ppat.1009382
482 Duvall LB, Ramos-Espiritu L, Barsoum KE, Glickman JF, Vosshall LB. 2019. Small-Molecule
483 Agonists of Ae. aegypti Neuropeptide Y Receptor Block Mosquito Biting. *Cell* **176**:687-
484 701.e5. doi:10.1016/j.cell.2018.12.004
485 Fiorenzano JM, Koehler PG, Xue R De. 2017. Attractive toxic sugar bait (ATSB) for control of
486 mosquitoes and its impact on non-target organisms: A review. *Int J Environ Res Public*
487 *Health* **14**. doi:10.3390/ijerph14040398
488 Galun R. 1963. Feeding Response in Aedes aegypti: Stimulation by Adenosine Triphosphate.
489 *Science (80-)* **142**:1674–1675. doi:10.1126/science.142.3600.1674
490 Garczynski SF, Crim JW, Brown MR. 2005. Characterization of neuropeptide F and its
491 receptor from the African malaria mosquito, Anopheles gambiae. *Peptides* **26**:99–107.

492 doi:10.1016/j.peptides.2004.07.014
493 González-Morales MA, Thomson AE, Yeatts J, Enomoto H, Haija A, Santangelo RG, Petritz
494 OA, Crespo R, Schal C, Baynes R. 2023. Pharmacokinetics of fluralaner as a systemic
495 drug to control infestations of the common bed bug, Cimex lectularius, in poultry facilities.
496 *Parasites and Vectors* **16**:1–8. doi:10.1186/s13071-023-05962-3
497 Gulia-Nuss M, Nuss AB, Meyer JM, Sonenshine DE, Roe RM, Waterhouse RM, Sattelle DB,
498 De La Fuente J, Ribeiro JM, Megy K, Thimmapuram J, Miller JR, Walenz BP, Koren S,
499 Hostetler JB, Thiagarajan M, Joardar VS, Hannick LI, Bidwell S, Hammond MP, Young S,
500 Zeng Q, Abrudan JL, Almeida FC, Ayllón N, Bhide K, Bissinger BW, Bonzon-Kulichenko
501 E, Buckingham SD, Caffrey DR, Caimano MJ, Croset V, Driscoll T, Gilbert D, Gillespie JJ,
502 Giraldo-Calderón GI, Grabowski JM, Jiang D, Khalil SMS, Kim D, Kocan KM, Koči J, Kuhn
503 RJ, Kurtti TJ, Lees K, Lang EG, Kennedy RC, Kwon H, Perera R, Qi Y, Radolf JD,
504 Sakamoto JM, Sánchez-Gracia A, Severo MS, Silverman N, Šimo L, Tojo M, Tornador C,
505 Van Zee JP, Vázquez J, Vieira FG, Villar M, Wespiser AR, Yang Y, Zhu J, Arensburger P,
506 Pietrantonio P V., Barker SC, Shao R, Zdobnov EM, Hauser F, Grimmelikhuijzen CJP,
507 Park Y, Rozas J, Benton R, Pedra JHF, Nelson DR, Unger MF, Tubio JMC, Tu Z,
508 Robertson HM, Shumway M, Sutton G, Wortman JR, Lawson D, Wikel SK, Nene VM,
509 Fraser CM, Collins FH, Birren B, Nelson KE, Caler E, Hill CA. 2016. Genomic insights into
510 the Ixodes scapularis tick vector of Lyme disease. *Nat Commun* **7**.
511 doi:10.1038/ncomms10507
512 Hamamoto H, Tonoike A, Narushima K, Horie R, Sekimizu K. 2009. Silkworm as a model
513 animal to evaluate drug candidate toxicity and metabolism. *Comp Biochem Physiol - C*
514 *Toxicol Pharmacol* **149**:334–339. doi:10.1016/j.cbpc.2008.08.008
515 Hammond A, Galizi R, Kyrou K, Simoni A, Siniscalchi C, Katsanos D, Gribble M, Baker D,
516 Marois E, Russell S, Burt A, Windbichler N, Crisanti A, Nolan T. 2016. A CRISPR-Cas9
517 gene drive system targeting female reproduction in the malaria mosquito vector
518 Anopheles gambiae. *Nat Biotechnol* **34**:78–83. doi:10.1038/nbt.3439
519 Harder E, Damm W, Maple J, Wu C, Reboul M, Xiang JY, Wang L, Lupyan D, Dahlgren MK,
520 Knight JL, Kaus JW, Cerutti DS, Krilov G, Jorgensen WL, Abel R, Friesner RA. 2016.
521 OPLS3: A Force Field Providing Broad Coverage of Drug-like Small Molecules and
522 Proteins. *J Chem Theory Comput* **12**. doi:10.1021/acs.jctc.5b00864
523 He Y, Xu X, Qiu J, Yin W, Sima Y, Xu S. 2020. Bombyx mori used as a fast detection model of
524 liver melanization after a clinical drug – Acetaminophen exposure. *J Asia Pac Entomol*
525 **23**:177–185. doi:10.1016/j.aspen.2019.11.009
526 Inui A. 1999. Feeding and body-weight regulation by hypothalamic neuropeptides - Mediation
527 of the actions of leptin. *Trends Neurosci* **22**:62–67. doi:10.1016/S0166-2236(98)01292-2
528 Judson CL. 1967. Feeding and oviposition behavior in the mosquito Aedes aegypti (L.).I.
529 Preliminary studies of physiological control mechanisms. *Biol Bull* **133**:369–377.
530 doi:10.2307/1539832
531 Khalak Y, Tresadern G, Aldeghi M, Baumann HM, Mobley DL, de Groot BL, Gapsys V. 2021.
532 Alchemical absolute protein-ligand binding free energies for drug design. *Chem Sci*
533 **12**:13958–13971. doi:10.1039/d1sc03472c
534 Klowden MJ. 1981. Initiation and Termination of Host-Seeking **27**:799–803. doi:10.1016/0022-
535 1910(81)90071-8.
536 Klowden MJ, Lea A. 1979a. Humoral inhibition of host seeking in Aedes aegypti during oocyte
537 maturation **25**. doi:doi:10.1016/0022-1910(79)90048-9

538 Klowden MJ, Lea AO. 1979b. Abdominal distention terminates subsequent host-seeking
539 behaviour of Aedes aegypti following a blood meal. *J Insect Physiol* **25**:583–585.
540 doi:10.1016/0022-1910(79)90073-8
541 Kraemer MU, Sinka ME, Duda KA, Mylne AQ, Shearer FM, Barker CM, Moore CG, Carvalho
542 RG, Coelho GE, Van Bortel W, Hendrickx G, Schaffner F, Elyazar IR, Teng H-J, Brady
543 OJ, Messina JP, Pigott DM, Scott TW, Smith DL, William Wint G, Golding N, Hay SI.
544 2015. The global distribution of the arbovirus vectors Aedes aegypti and Ae. albopictus.
545 *Elife*. doi:10.7554/eLife.08347.001
546 Krockel U, Rose A, Eiras AE, Geier M. 2006. New tools for surveillance of adult yellow fever
547 mosquitoes: comparison of trap catches with human landing rates in an urban
548 environment. *J Am Mosq Control Assoc* **22**:229–38. doi:10.2987/8756-
549 971X(2006)22[229:NTFSOA]2.0.CO;2
550 Kuenzel WJ, Douglass LW, Davison BA. 1987. Robust feeding following central administration
551 of neuropeptide Y or peptide YY in chicks, Gallus domesticus. *Peptides* **8**:823–828.
552 doi:10.1016/0196-9781(87)90066-0
553 Lees RS, Gilles JR, Hendrichs J, Vreysen MJ, Bourtzis K. 2015. Back to the future: the sterile
554 insect technique against mosquito disease vectors. *Curr Opin Insect Sci* **10**:156–162.
555 doi:10.1016/j.cois.2015.05.011
556 Liesch J, Bellani LL, Vosshall LB. 2013. Functional and Genetic Characterization of
557 Neuropeptide Y-Like Receptors in Aedes aegypti. *PLoS Negl Trop Dis* **7**:e2486.
558 doi:10.1371/journal.pntd.0002486
559 Liu N. 2015. Insecticide resistance in mosquitoes: Impact, mechanisms, and research
560 directions. *Annu Rev Entomol* **60**:537–559. doi:10.1146/annurev-ento-010814-020828
561 Macias VM, Ohm JR, Rasgon JL. 2017. Gene drive for mosquito control: Where did it come
562 from and where are we headed? *Int J Environ Res Public Health* **14**.
563 doi:10.3390/ijerph14091006
564 Moyes CL, Vontas J, Martins AJ, Ng LC, Koou SY, Dusfour I, Raghavendra K, Pinto J, Corbel
565 V, David JP, Weetman D. 2021. Correction to: Contemporary status of insecticide
566 resistance in the major aedes vectors of arboviruses infecting humans (PLoS Negl Trop
567 Dis). *PLoS Negl Trop Dis* **15**:1–2. doi:10.1371/journal.pntd.0009084
568 Mukabana WR, Mweresa CK, Otieno B, Omusula P, Smallegange RC, van Loon JJA, Takken
569 W. 2012. A Novel Synthetic Odorant Blend for Trapping of Malaria and Other African
570 Mosquito Species. *J Chem Ecol* **38**:235–244. doi:10.1007/s10886-012-0088-8
571 Okumu FO, Killeen GF, Ogoma S, Biswaro L, Smallegange RC, Mbeyela E, Titus E, Munk C,
572 Ngonyani H, Takken W, Mshinda H, Mukabana WR, Moore SJ. 2010. Development and
573 field evaluation of a synthetic mosquito lure that is more attractive than humans. *PLoS*
574 *One* **5**. doi:10.1371/journal.pone.0008951
575 Parihar K, Telang M, Ovhal A. 2020. A patent review on strategies for biological control of
576 mosquito vector. *World J Microbiol Biotechnol* **36**:1–23. doi:10.1007/s11274-020-02960-w
577 Qiu H, Jun HW, Tao J. 1997. Pharmacokinetics of insect repellent N,N-diethyl-m-toluamide in
578 beagle dogs following intravenous and topical routes of administration. *J Pharm Sci*
579 **86**:514–516. doi:10.1021/js960283m
580 Ryan SJ, Carlson CJ, Mordecai EA, Johnson LR. 2019. Global expansion and redistribution of
581 Aedes -borne virus transmission risk with climate change. *PLoS Negl Trop Dis* **13**:1–20.
582 doi:https://doi.org/10.1371/journal.pntd.0007213
583 Savino F, Ricciardi R, Iodice A, Benelli G, Conte G, Lucchi A, Ladurner E, Cosci F. 2018. Eco-

584 friendly pheromone dispensers—a green route to manage the European grapevine moth?
585 *Environ Sci Pollut Res* **25**:9426–9442. doi:10.1007/s11356-018-1248-3
586 Su X, Guo Y, Deng J, Xu J, Zhou G, Zhou T, Li Y, Zhong D, Kong L, Wang X, Liu M, Wu K,
587 Yan G, Chen XG. 2019. Fast emerging insecticide resistance in Aedes albopictus in
588 Guangzhou, China: Alarm to the dengue epidemic. *PLoS Negl Trop Dis* **13**:1–15.
589 doi:10.1371/journal.pntd.0007665
590 Weaver SC, Costa F, Garcia-Blanco MA, Ko AI, Ribeiro GS, Saade G, Shi PY, Vasilakis N.
591 2013. Zika virus: History, emergence, biology, and prospects for control. *PLoS One* **13**:1–
592 15. doi:10.1155/2017/3196924
593 Witmer GW, Raymond-Whish S, Moulton RS, Pyzyna BR, Calloway EM, Dyer CA, Mayer LP,
594 Hoyer PB. 2017. Compromised Fertility in Free Feeding of Wild-Caught Norway Rats (
595 Rattus Norvegicus) With a Liquid Bait Containing 4-Vinylcyclohexene Diepoxide and
596 Triptolide. *J Zoo Wildl Med* **48**:80–90. doi:10.1638/2015-0250.1
597 World Health Organization. 2012. Global Plan for Insecticide Resistance Management in
598 Malaria Vectors. Geneva, Swizterland. doi:WHO REFERENCE NUMBER:
599 WHO/HTM/GMP/2012.5
600 Wu Q, Wen T, Lee G, Park JH, Cai HN, Shen P. 2003. Developmental control of foraging and
601 social behavior by the Drosophila neuropeptide Y-like system. *Neuron* **39**:147–161.
602 doi:10.1016/S0896-6273(03)00396-9
603 Zhang J, Yang J, Jang R, Zhang Y. 2015. GPCR-I-TASSER: A Hybrid Approach to G Protein-
604 Coupled Receptor Structure Modeling and the Application to the Human Genome.
605 *Structure* **23**:1538–1549. doi:10.1016/j.str.2015.06.007
606